Active surface salt structures of the western Kuqa fold-thrust belt, northwestern China

Jianghai Li[1], A. Alexander G. Webb[2,*], Xiang Mao[1], Ingrid Eckhoff[2], Cindy Colón[2], Kexin Zhang[2], Honghao Wang[1], An Li[2], and Dian He[2,†]

[1]*The Key Laboratory of Orogenic Belts and Crustal Evolution, Ministry of Education, School of Earth and Space Sciences, Peking University, Beijing 100871, China*

[2]*Department of Geology and Geophysics, Louisiana State University, Baton Rouge, Louisiana 70803, USA*

ABSTRACT

The western Kuqa fold-thrust belt of Xinjiang Province, China, hosts a series of surface salt structures. Here we present preliminary analysis of the geometry, kinematics, and surface processes of three of these structures: the Quele open-toed salt thrust sheet, Tuzimazha salt wall, and Awate salt fountain. The first two are line-sourced, the third appears to be point-sourced, and all are active. The ~35-km-long, 200-m-thick Quele open-toed salt thrust sheet features internal folding, salt-lined transfer structures, dissolution topography, flanking growth strata, and alluvial fan/stream-network interactions. The ~10-km-long, 50-m-wide Tuzimazha salt wall marks a local topographic high, such that fluvial stream networks are deflected by the rising weak tabular salt body. The salt wall is also flanked by growth strata and normal faults. The ~2-km-long Awate salt fountain represents salt exhumation coincident with the intersection of multiple structures and a river. Therefore this salt body may respond to local structural and/or erosional variations, or it may play a key role determining such variations—or both. Activity along all three structures confirms that active deformation occurs from foreland to hinterland across the western Kuqa fold-thrust belt. Gradual lateral transition from bedded strata to flow-banded halite observed within the Quele open-toed salt thrust sheet implies that similar transitions observed in seismic reflection data do not require interpretation as diapiric cut-off relationships. The surface salt structures of the western Kuqa fold-thrust belt display a variety of erosion-tectonics interactions, with nuances reflecting the low viscosity and high erodibility of salt, including stream deflections, potential tectonic aneurysm development, and even an upper-crustal test site for channel flow–focused denudation models.

INTRODUCTION

Among common solid Earth materials, salt is distinguished by uncommonly low density, low viscosity, near incompressibility, high solubility, and high thermal expansivity. Because of these distinctive attributes, salt and salt structures impact a variety of research: (1) Salt is a strong control on the evolution and deformation of many passive margin sequences, fold-thrust belts, rift basins, and interior basins (e.g., Letouzey et al., 1995; McClay et al., 2004; Rowan and Vendeville, 2006; Warren, 2006; Hudec and Jackson, 2007), which are settings that host the majority of oil and gas giants (Mann et al., 2003). (2) Salt layers make effective seals in petroleum traps, and large, partially evacuated salt bodies are used to store a variety of materials including hazardous waste (Thoms and Gehle, 2000; Dribus et al., 2008). (3) Salt is an analog material for studies of fluid dynamics across Earth's deep interior (Spetzler and Anderson, 1968; Jin et al., 1994). (4) Brine flows, diapiric domes, and other potential salt (or salt-analog) structures are recognized on Venus and Mars, so salt studies can offer insights into material flow and the cycling of water on planets and moons (e.g., McKenzie et al., 1992; Montgomery et al., 2009; McEwen et al., 2011).

The diverse economic and research benefits of salt studies highlight the importance of exploring salt occurrences at the Earth surface, where their geometries and internal structures can be directly observed and used to constrain the dynamics of salt motion. Although geoscientists have interpreted thousands of salt sheets in more than 35 basins worldwide (Hudec and Jackson, 2006, 2007), subaerial preservation of halite salt structures is rare (Talbot and Pohjola, 2009; Barnhart and Lohman, 2012). A fraction of these subaerial salt structures occur in active settings, where boundary conditions of ongoing deformation can be geodetically characterized.

The Kuqa fold-thrust belt of Xinjiang Province, northwestern China, offers a new prospect for subaerial investigation of a range of active salt structures. Because the Kuqa fold-thrust belt hosts numerous gas giants and other plays (e.g., Zhao et al., 2005), it has been explored extensively via wells, seismic reflection, and balanced palinspastic reconstruction. Over the past decade, this research has shown that salt deformation controls ongoing construction of the fold-thrust belt (e.g., Tang et al., 2004; Wang et al., 2011). We have initiated a new research effort focusing on the western part of the Kuqa fold-thrust belt where salt reaches the surface in multiple structural settings. Our preliminary field work and satellite image analysis confirm surface outcrops of active salt structures, including the salt thrust sheets, salt walls, and salt namakiers ("glaciers" of salt; see Talbot and Pohjola, 2009). Here we provide initial geometric and kinematic characterization of these structures and their relationships to erosive processes.

GEOLOGIC BACKGROUND

The Kuqa fold-thrust belt accommodates active north-south shortening across a ~400-km-long, ~20–65-km-wide area (Fig. 1) (Zhong and Xia, 1998). This belt forms a segment of the topographic front separating the Tian Shan (i.e., Celestial Mountains) to the north from the Tarim basin to the south. Deformation occurs

*Corresponding author: awebb@lsu.edu

†Present address: Shell International Exploration and Production Inc., 3333 Hwy 6 South, Houston, Texas 77082, USA

Geosphere; December 2014; v. 10; no. 6; p. 1219–1234; doi:10.1130/GES01021.1; 9 figures.

Received 29 December 2013 ♦ Revision received 18 July 2014 ♦ Accepted 4 September 2014 ♦ Published online 15 October 2014

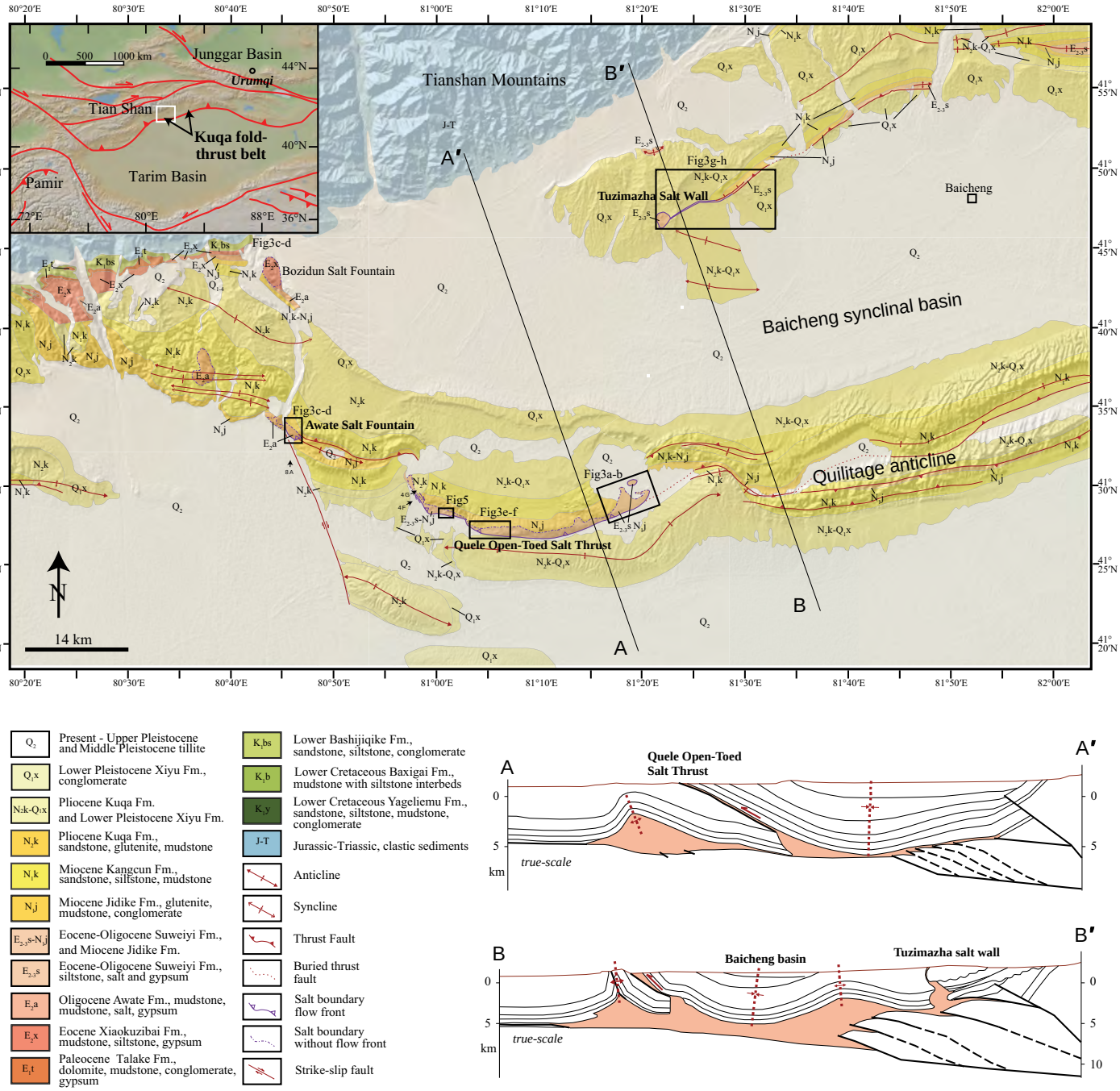

Figure 1. Geologic map of the western Kuqa fold-thrust belt. Inset shows the location of the Kuqa fold-thrust belt along the southern margin of the Tian Shan and the northern edge of the Tarim basin. Cross-section lines are adapted from Li et al. (2012). Figure locations are indicated with rectangles (maps) and arrows (photographs). The Awate, Xiaokuzibai, and Talake Formations together form the Kumugeliemu Group.

as a far-field effect of India-Asia collision and has been ongoing and accelerating since the latest Oligocene (e.g., Molnar and Tapponnier, 1975; Allen et al., 1991; Yin et al., 1998; Wang et al., 2011; Craig et al., 2012). Global positioning system (GPS) velocity studies indicate that the Tarim basin is being thrust beneath the Tian Shan at ~4–7 mm/yr (Wang et al., 2001; Zubovich et al., 2010). Balanced palinspastic reconstruction suggests that such convergence rates have persisted for the past ~2.5 million years across the Kuqa fold-thrust belt (Li et al., 2012).

The deformed rocks of the Kuqa fold-thrust belt almost exclusively represent Mesozoic–Cenozoic continental clastic sediments (e.g., Chen et al., 2004; Wang et al., 2011). A semi-continuous depositional record across this time interval is punctuated by a few gaps marked by unconformities and overlying conglomerates, with the longest gap (across the mid-Cretaceous) spanning ~45 million years (Peng et al., 2006; Wang et al., 2011). Mesozoic strata contain largely conglomerate, sandstones, siltstones, and mudstones, with some coal layers restricted

to the Lower to Middle Jurassic (Hendrix et al., 1992; Zhong and Xia, 1998). Cenozoic strata are up to ~7000 m thick, and in general, these sediments coarsen upwards (Fig. 2) (e.g., Huang et al., 2006; Hubert-Ferrari et al., 2007; Wang et al., 2011). Paleogene–early Miocene sedimentary rocks are mudstones, siltstones, and evaporites; middle Miocene–Pliocene sequences feature sandstones and mudstones; and Quaternary sediments are dominated by gravels. Corresponding sedimentary environments are interpreted to evolve from marginal marine–shallow lake–lagoon settings to river floodplains and alluvial fans (e.g., Zhong and Xia, 1998). Evaporite layers include the Paleogene Suweiyi Formation and Kumugeliemu Group in the western Kuqa fold-thrust belt, which features rock salt, gypsum, anhydrite, and dolomite interbedded with mudstone and shale, and the early Miocene Jidike Formation, which contains the same lithologies farther east (e.g., Tang et al., 2004; Li et al., 2012). Effects of salt flow on sedimentation patterns increase through time, such that pre-Pliocene strata form approximately parallel layers, whereas subsequent strata form increasingly pronounced growth strata and halokinetic sequences (cf. Giles and Rowan, 2012) during growth of salt diapirs, walls, and anticlines (Chen et al., 2004; Tang et al., 2004; Charreau et al., 2006; Sun et al., 2009; Wang et al., 2011; Li et al., 2012).

The structural framework of the Kuqa fold-thrust belt can be divided into four components from north to south: a northern contractional belt, the Baicheng syncline, the Quilitage anticline system, and frontal detachment anticlines (Fig. 1) (Yin et al., 1998; Wang et al., 2011). Deformation across all components largely postdates the late Miocene, is active, and is strongly influenced by salt (Chen et al., 2004; Li et al., 2012). In the northern contractional belt, thrust stacking of Mesozoic rocks at depth is partially decoupled from salt-influenced shortening of Cenozoic rocks above. Farther south, the salt horizons form the basal detachments. Salt is partially expelled below the depocenter formed by the Baicheng syncline, which is largely filled with growth strata (e.g., Li et al., 2012). The Quilitage anticline system represents a series of folds and associated thrusts that grew along the southern flank of the Baicheng syncline (He and Li, 2009); the Quele open-toed salt thrust sheet is a western portion of this system. Farther south, detachment folds cored with salt separate the fold-thrust belt from the Tarim basin. North-trending strike-slip faults impart local limits on lateral fold growth throughout the Kuqa fold-thrust belt (e.g., Zhong and Xia, 1998).

SURFACE SALT STRUCTURES

Although salt tectonics dominates the regional deformation patterns, salt surface exposures are largely restricted to the western Kuqa fold-thrust belt (Fig. 1) (Zhong and Xia, 1998; Wang et al., 2011; Li et al., 2012). Here

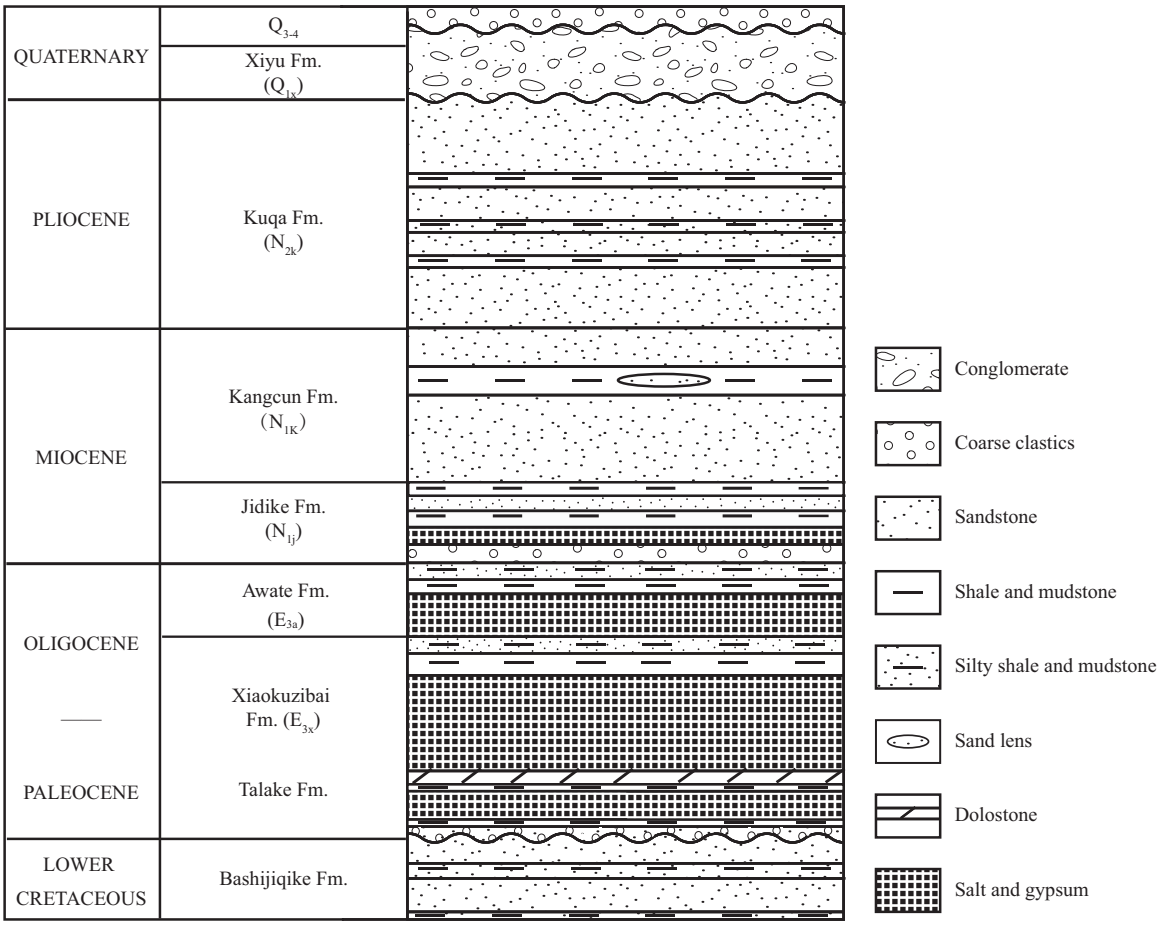

Figure 2. Stratigraphic column of the western Kuqa fold-thrust belt from latest Mesozoic to present, adapted from Chen et al. (2004) and Wang et al. (2011). The Awate, Xiaokuzibai, and Talake Formations together form the Kumugeliemu Group.

the evaporites of the Kumugeliemu Group occur at point-sourced salt fountains and line-sourced structures. Most of the surface salt structures feature active uplift, exhumation, and surface flow of salt. Salt structures display a variety of materials, with mixtures including various proportions of flow-banded halite, blocks and veins of gypsum, and highly oxidized mudrock. Common topographic characteristics include distinctive steepening profiles at the leading edges of advancing namakiers, dissolution features at scales ranging up to tens of meters, and prominent m-scale mounds reflecting preferential preservation of gypsum. Structural geometries at km to mm scale are generally correlated with drainage network morphologies. Here we focus on the surface characteristics of three salt structures: the Quele open-toed salt thrust sheet, the Tuzimazha salt wall, and the Awate salt fountain (Figs. 1 and 3).

Quele Open-Toed Salt Thrust Sheet

One of Earth's most spectacular open-toed salt thrust sheets marks the surface expression of the active Quele thrust (Figs. 4A–4C). The salt thrust sheet is exposed ~60 km to the west-southwest of the city of Baicheng, and it dominates a ~35-km-long range front with salt masses up to ~200 m thick (Figs. 1, 3A, 3B, 3E, and 3F). The salt feeding the open-toed salt thrust sheet is exhumed along the south-directed, north-dipping Quele salt thrust, which extends down to the salt décollement horizon at ~7 km below the ground surface (Chen et al., 2004). The surface of the salt thrust sheet is generally smooth down to meter scale due to gravity spreading and water dissolution and steepens toward the flow front.

The activity of the open-toed salt thrust sheet system is indicated by the southwards flow of the salt over active depocenters and the eroding northern limb of the Misikantage anticline, a detachment fold (Figs. 4A–4C). Advance of the salt thrust sheet (i.e., southwards flow > removal via erosion and dissolution) is indicated by a lack of moraines (e.g., Fig. 4C); indeed no moraines are observed along any of the studied Kuqa salt structures. The character of the hanging wall changes along strike: along most segments, a ~200-m-thick salt thrust sheet and/or namakier without overlying strata is observed (Figs. 4A and 4B), but along some western portions the salt layer thins to ~50 m thick with overlying gypsum- and salt-bearing mudstone strata (Fig. 4C), and locally the salt pinches out such that only the bedded strata occur along the front (Fig. 4D). Transitions from bedded (clastic + evaporite) strata to flowing salt occur not only up and down section but also laterally (Fig. 4D), showing that only minor changes in Kumugeliemu Group lithology can allow flow. The mixed bedded-salt horizons locally contain 100-m-scale sheath folds (perhaps tank-track folds, cf. Talbot, 1998) indicative of southwards flow.

To the west, slip along the Quele salt thrust is transferred by a strike-slip fault (Fig. 1). A ≥30-m-wide exposure of salt occurs along the length of the strike-slip fault (Figs. 4F and 4G). Decimeter-scale growth strata that developed in river terrace deposits along the western margin of the salt suggest that the salt is extruding upwards along this structure. This upwelling salt likely lubricates the strike-slip fault. The Quele salt thrust and the strike-slip fault at its western termination may link with, or have a step-over relationship with, another thrust fault to the north that extends farther west.

To the east, the Quele open-toed salt thrust sheet widens to cover a ~5-km-wide region; this wide region is termed the Chaerhan namakier (Figs. 1, 3A, and 3B). Farther east, the namakier terminates, and the likely eastward extension of the fault is covered by active clastic deposition. Beneath the cover of the Chaerhan namakier and clastic sediment, there may be a strike-slip fault transferring slip to the north, since additional structures accommodate north-south contraction to the northeast. The Chaerhan namakier is triangular in map view, with an isolated salt fountain or klippe to the north (Figs. 3A and 3B). Growth strata marking salt uplift occur in the Miocene sediments along the western edge of the triangular namakier (Fig. 4H). A rich folding history, featuring tight-to-isoclinal folds and domes, is revealed within the Chaerhan namakier by alternations of white layers (halite-dominated) and red layers (mud-and-salt layers) (Figs. 3 and 4I). The low relief and dominant dissolution structures largely preclude determination of layer dips. Discontinuous gypsum-dominated layers represent ≤1% of the area of the Chaerhan namakier, commonly occur as local topographic highs, and in some cases can be used to measure dip. Also, a few isolated blocks of coherent sedimentary strata are preserved within the namakier and appear to be dominated by subvertical dips (Figs. 3 and 4J).

A series of decameter-scale and larger morphological features of the Quele open-toed salt thrust sheet are controlled by water erosion. Such large-scale dissolution and collapse topography is primarily evinced by caves (Fig. 4E). Along the portions of the range front where salt flows over active depocenters, these caves and the associated southward-flowing streams correlate to minima in the advance of the namakier (Fig. 5). Arcs of salt occur between each stream, and fans developed in front of the streams funnel minor channels into interfan drainages. Brittle slides accommodate collapse of the viscous flow front (Figs. 4A, 4B, and 5), and are particularly well developed along the portions of the range front where salt flows into canyons. Similar collapse structures occur along the southeastern margin of the isolated salt body at the northern limit of the Chaerhan namakier. Ephemeral lakes, which develop immediately to the south of the salt body, tend to concentrate water along this margin, and the resultant calving structures form a horst and graben system (Fig. 4K). (We borrow the term "calving structures" from glacial morphologies, in particular cases where a glacier terminates at a water body and its toe collapse occurs along structures that may be lubricated by the adjacent water body.)

Tuzimazha Salt Wall

To our knowledge, the Tuzimazha salt wall represents Earth's best developed active subaerial salt wall (Figs. 6A and 6B). Such features are rare: the only other active subaerial salt wall we are aware of is the strike-slip fault marking the western termination of the Quele salt thrust. Both structures are sufficiently thin (i.e., ≤50 m wide) that they may alternatively be termed incomplete salt welds (Hudec and Jackson, 2011), although the weld term is generally used to describe inactive structures. The Tuzimazha salt wall trends east-southeast across the hinterland of the western Kuqa fold-thrust belt for ~10 km (Figs. 3G and 3H). The wall is subvertical, rising up to ~30 m above local base level with a width of up to ~50 m in map view and is flanked on both sides by halokinetic growth strata (cf. Giles and Rowan, 2012) (Figs. 6A and 6B). The rocks immediately north of the salt wall also feature meter- to 100-m-scale, top-north normal faulting, which we interpret as kinematically consistent with the rise of the salt to the south (Figs. 6C and 6D). Map-view morphology of the salt wall is dominated by a kink in the center: an eastern east-trending segment and a western east-southeast–trending segment meet at a corner (Fig. 3). To the west, the structure appears to terminate at a point-source diapir with a 1-km-diameter surface expression (Fig. 3). This may be a half-"Q-tip" structure representing a concentration of shortening in the central portion of the salt wall (à la Rowan and Vendeville, 2006; Rowan et al., 2012); if so, it suggests that such structures may develop without terminating salt extrusion along the thin central segments. To the east, the salt wall transitions into a top-south thrust fault system featuring localized salt extrusions (Fig. 3).

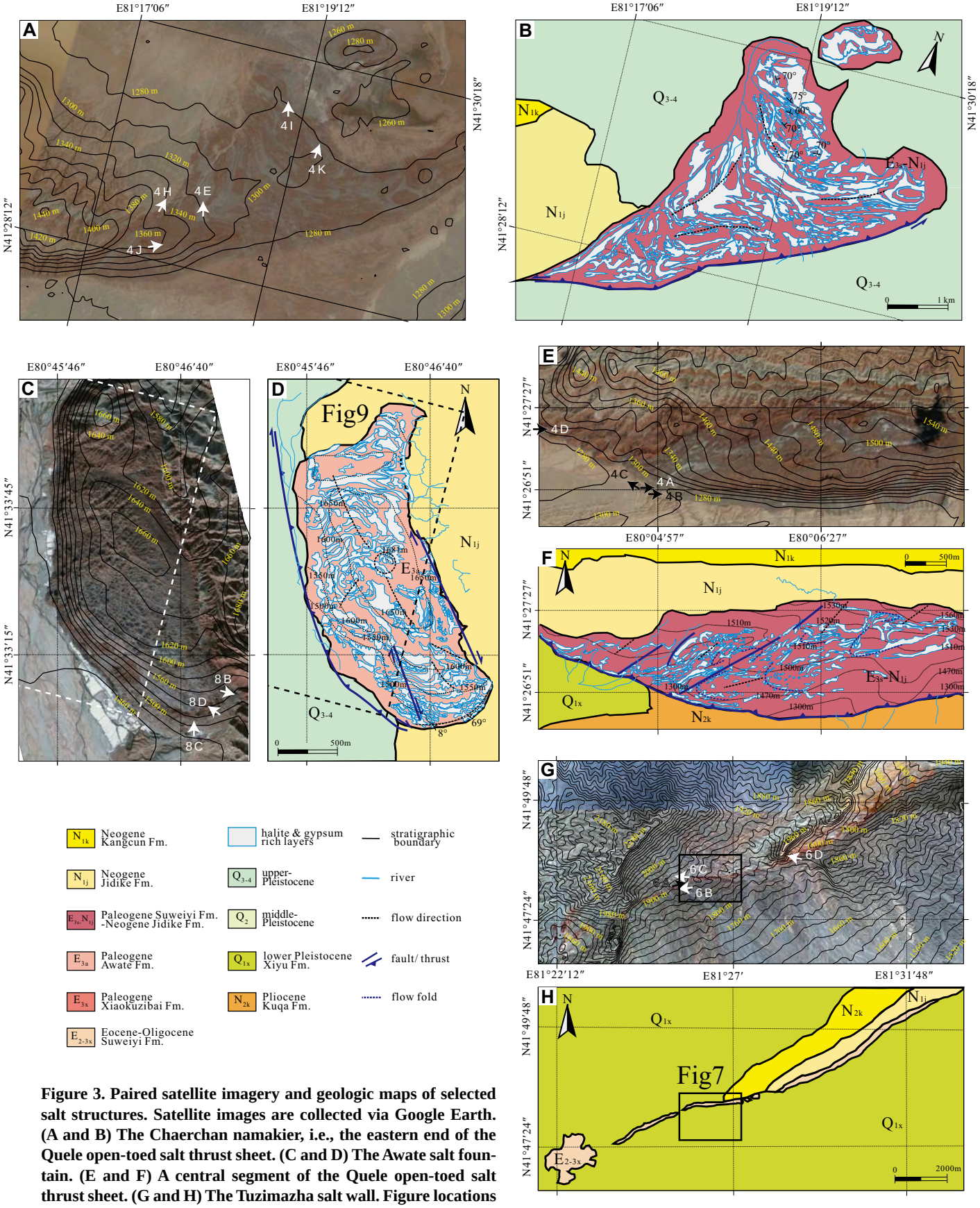

Figure 3. Paired satellite imagery and geologic maps of selected salt structures. Satellite images are collected via Google Earth. (A and B) The Chaerchan namakier, i.e., the eastern end of the Quele open-toed salt thrust sheet. (C and D) The Awate salt fountain. (E and F) A central segment of the Quele open-toed salt thrust sheet. (G and H) The Tuzimazha salt wall. Figure locations are indicated with rectangles (maps) and arrows (photographs).

Figure 4 (*on this and following two pages*). Photographs of key features of the Quele open-toed salt thrust sheet. Vantage points for photographs are indicated in Figures 1 and 3. (A) The salt thrust sheet front flowing into a rapidly developed canyon. Some drainages cut the front of the salt thrust sheet and show that its contact with the underlying pre-canyon basin fill is subhorizontal; so the salt flow must locally create a hanging wall flat on footwall flat geometry at the leading edge of the Quele salt thrust. (B) Here the salt front is flowing onto tilted bedding of the detachment fold to the south of the Quele salt thrust. (C) In the west, the salt front is adjacent to a subhorizontal basin. (D) Flowing salt-and-mud laterally transitions to coherent salt-and-mud strata over a distance of ~200 m along the Quele open-toed salt thrust sheet front. Heavy dashed line indicates the leading edge of the salt thrust sheet. (E) A cave developed by water flow and dissolution of salt. This photograph highlights the care that must be exercised working on salt: a person walking (south)-east might not see this cave until a step or two prior to entering it.

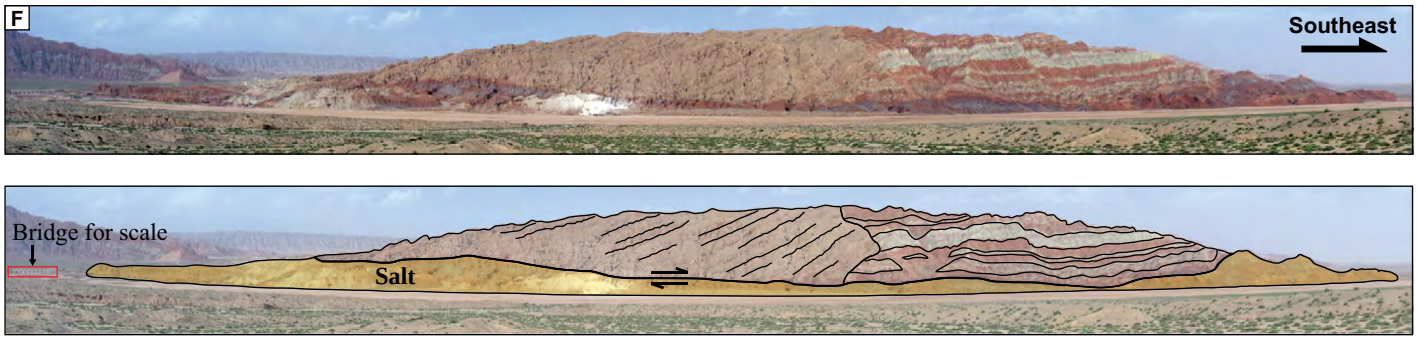

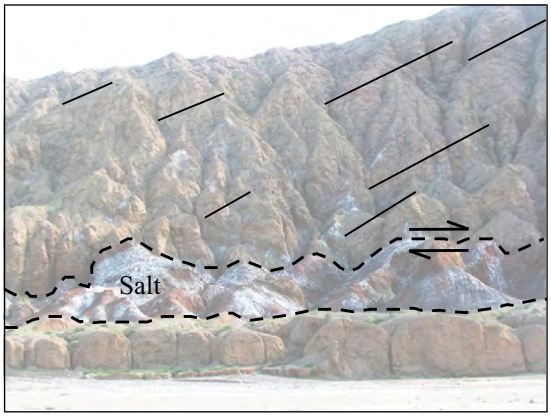

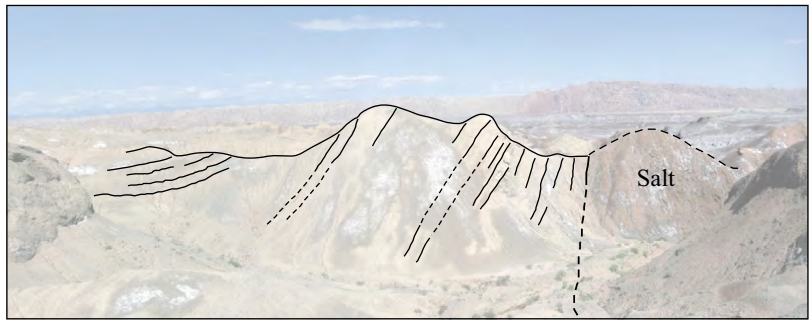

Figure 4 (*continued*). (F) Kilometer-scale photograph of the salt strike-slip fault forming the western termination of the Quele open-toed salt thrust sheet. Note that the salt appears concordant with the strata to the southeast, but these strata are capped by another sequence across an unconformity, and the higher sequence is cut by the strike-slip fault. (G) Decameter-scale photograph of the salt strike-slip fault forming the western termination of the Quele open-toed salt thrust sheet. Bedding terminates along the salt-lined fault zone. (H) Growth strata adjacent to the Chaerchan namakier marking the eastern termination of the Quele open-toed salt thrust sheet. Strata dips steeply adjacent to the salt, but shallowly ~50 m away from the salt. (I) Folding in the Chaerchan namakier (i.e., the eastern termination of the Quele open-toed salt thrust sheet). The inset shows a satellite image of the same area, with the folds noted in both the photograph and satellite image marked in blue and additional folds visible in the satellite image marked with cyan. (J) Isolated coherent strata within the Chaerchan namakier (i.e., the eastern termination of the Quele open-toed salt thrust sheet). (K) Calving of an isolated salt dome just east of the Quele open-toed salt thrust sheet. Three major calving faults are highlighted in black, pink, and red. The inset shows a satellite image of the same area, annotated with the same colors. The calving structures appear spatially correlated with areas that commonly host ephemeral waters. We surmise that local weakening of the salt dome via uptake of ephemeral water produces calving.

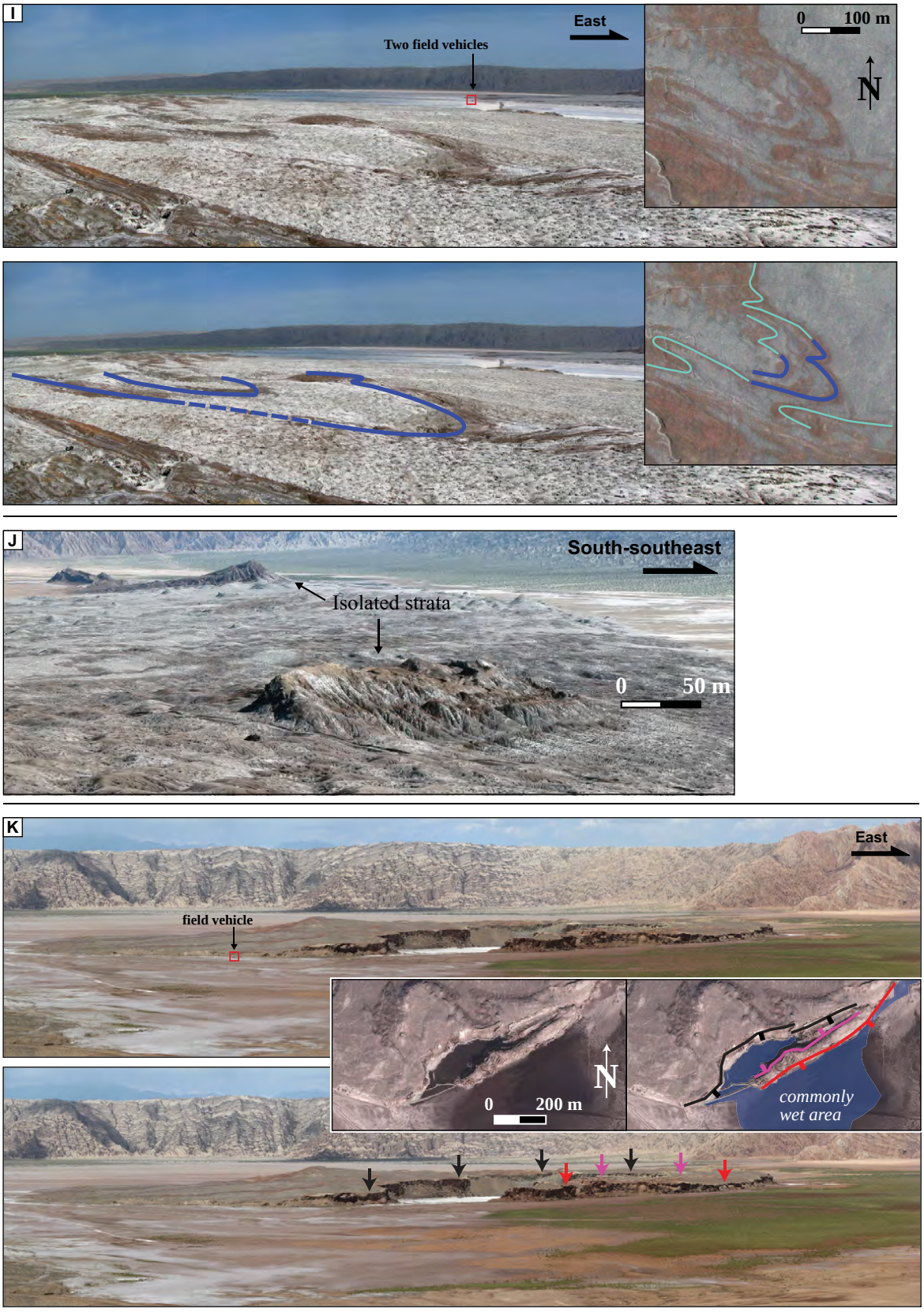

Figure 4 (*continued*).

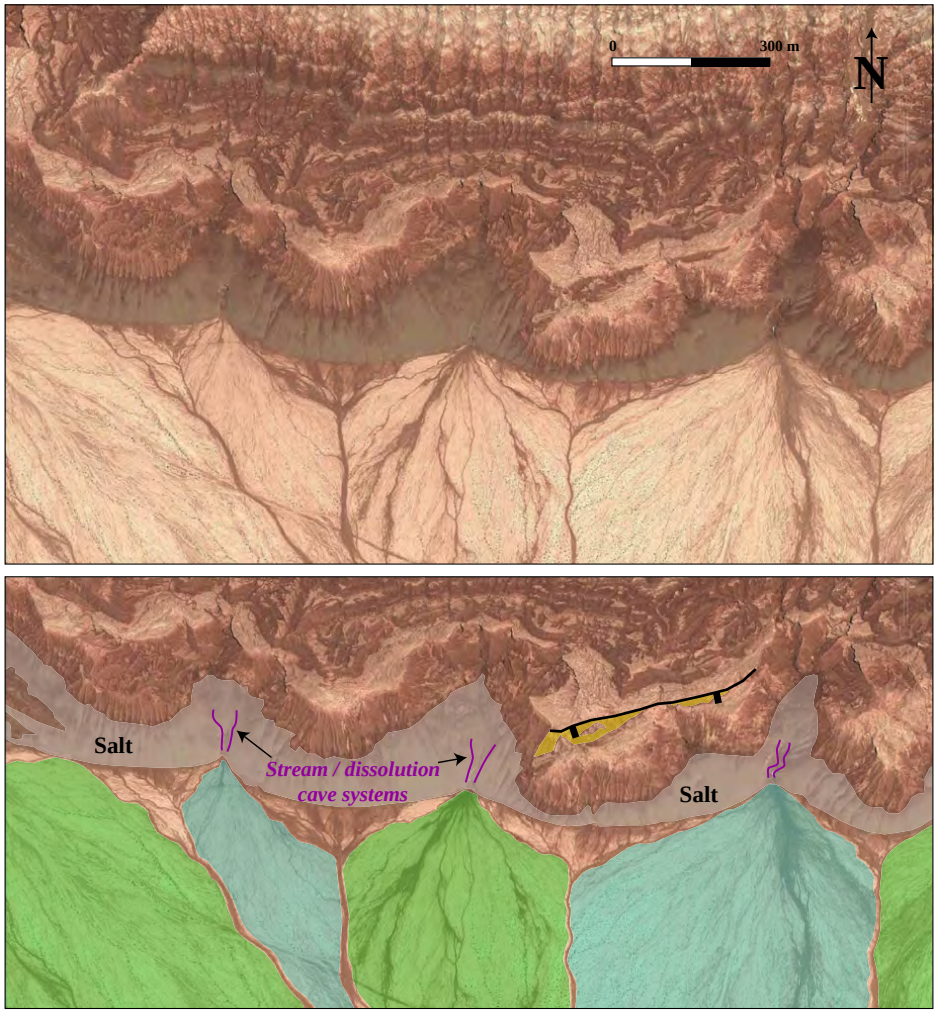

Figure 5. Satellite image showing the correlations between the salt, stream, and fan geometries along the front of the Quele open-toed salt thrust sheet. Where the salt thrust sheet (pale shading in the annotated figure) flows over subhorizontal active depocenters, a regular morphological pattern develops. The largest streams flowing southwards from the salt thrust sheet commonly form dissolution morphologies, such that some parts of the streams flow through the namakiers in caves (southern portions of stream/cave systems are marked in purple). The outflows of these streams at the southern limit of the salt thrust sheet correlate with minima in the advance of the salt, such that the areas between streams show convex-southwards fronts. Directly south of each large stream, an alluvial fan develops (marked in blues and greens). The topography of these fans funnels all smaller streams exiting the open-toed salt thrust sheet into interfan stream systems, which commonly merge into a single interfan drainage less than ~100 m south of the salt (a similar pattern can be observed at 100-km scale between Himalayan megafans). A local collapse of the salt thrust sheet overburden occurs in the eastern portion of the image. The break-away and exposed fault plane are highlighted in black and yellow.

Most of the area traversed by the Tuzimazha salt wall is experiencing fluvial erosion, with deposition limited to the beds of large streams. In this context, it is clear that salt exhumation is active because the salt forms a local high ridge despite its high erosive potential versus the surrounding continental strata (Figs. 6A and 6B). The uplift and exhumation of the salt wall and adjacent growth strata are also imprinted on aspects of the stream network morphology. Stream flow is generally from northwest to southeast, and large streams cross (and locally obliterate) the salt wall without deflection (Fig. 7). However, immediately to the east of the corner in the central portion of the salt wall, small streams are deflected eastwards along the ridges formed by salt and steeply tilted growth strata within ~50 m of the salt (Fig. 7). Approximately 400 m east of the corner, the local ridge line shifts southwards from the salt to steeply dipping growth strata ~50 m south of the salt wall, such that small streams flow northwards from this ridge across the salt wall. These streams collect in the east-flowing drainage north of the salt wall, and farther east this drainage merges with a larger stream and breaches southeastwards across the salt and proximal growth strata.

Awate Salt Fountain

The Awate salt fountain occurs in the far-western Kuqa fold-thrust belt, west of the Baicheng basin and within the western end of the Quilitage anticline system (Figs. 1, 3C, 3D, and 8A). It is roughly oval shaped in map view, with a length of ~2 km to the northwest, width of ~1 km, and elevation of ~200 m above the local base level (Figs. 3C and 3D). The surface of the Awate salt fountain is generally smooth down to meter scale due to gravity spreading and water dissolution. This pattern is disrupted along the western edge of the salt fountain, where water from an adjacent river results in calving and a steep range front, and the southern front at sites of salt mining activity (Figs. 3 and 9). A smaller salt body on the west side of the river may emanate from the same source, such that division of the salt bodies is accomplished via river erosion and fill (Fig. 1).

The restricted spatial extent of the Awate salt fountain suggests that the salt may rise along a linear conduit (i.e., a point-source interpretation), but the specifics of the structural setting are unclear. The salt fountain occurs along a northwest-trending, south-directed thrust fault that is lined with a ~5-m-thick salt layer (Fig. 8B); so this thrust horizon is the most likely source of the salt. Three end-member hypotheses may explain the concentration of salt exhumation along the thrust at the specific longitude of the Awate salt fountain: (1) enhanced erosion by the south-flowing river may preferentially exhume material; (2) the northernmost segment of a north-trending strike-slip fault may intersect the thrust fault, creating a steep linear zone of weakness exploited by the rising salt; and (3) salt uplift and exhumation may have initiated within a diapir prior to deposition of most surrounding strata, such that the rise of the diapir influenced the development of the structural and surface process systems.

The salt mining operations at the southern end of the Awate salt fountain commonly generate fresh outcrops at which internal structural

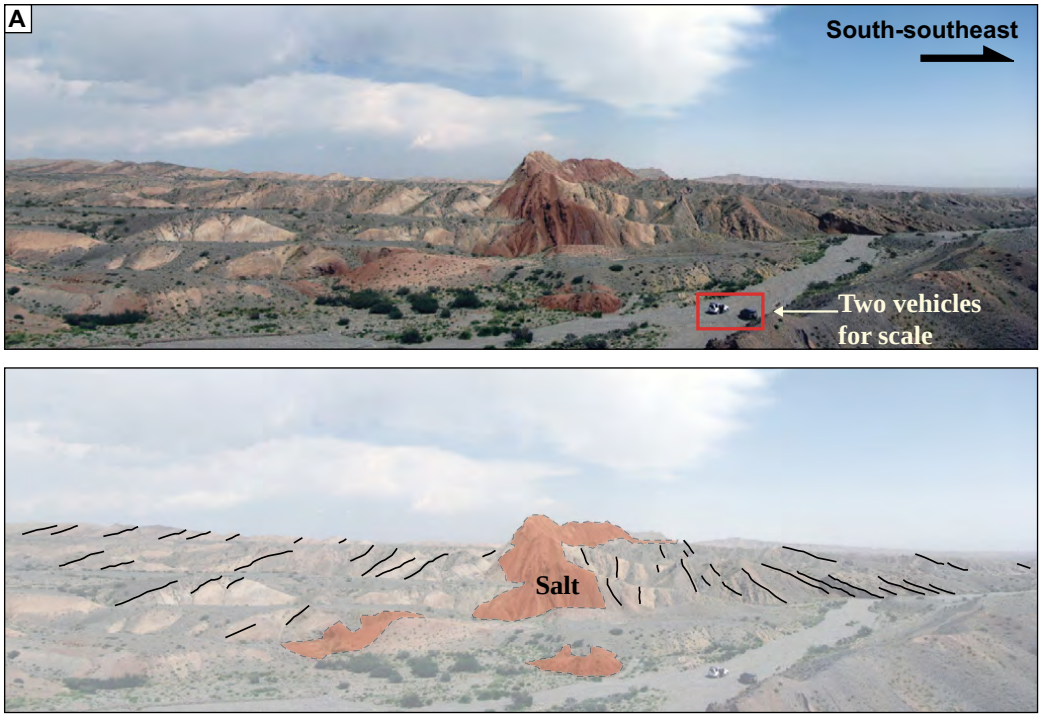

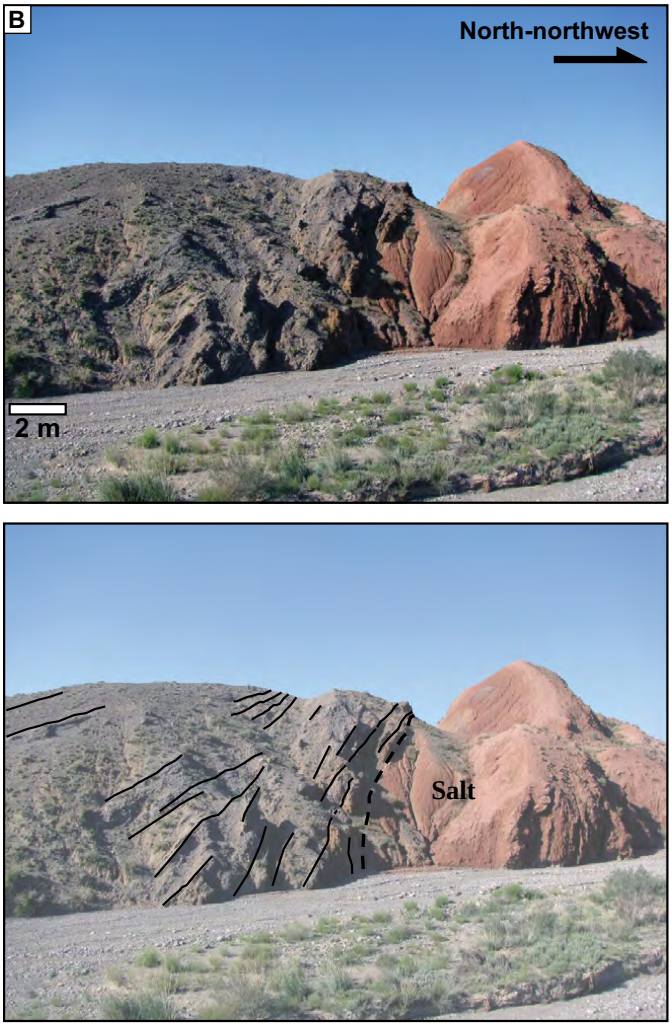

Figure 6 (*on this and following page*). Photographs of key features of the Tuzimazha salt wall. Vantage points for photographs are indicated in Figure 3. (A) The high ridge of the salt wall flanked by halokinetic growth strata. (B) Halokinetic growth strata along the southern margin of the salt wall.

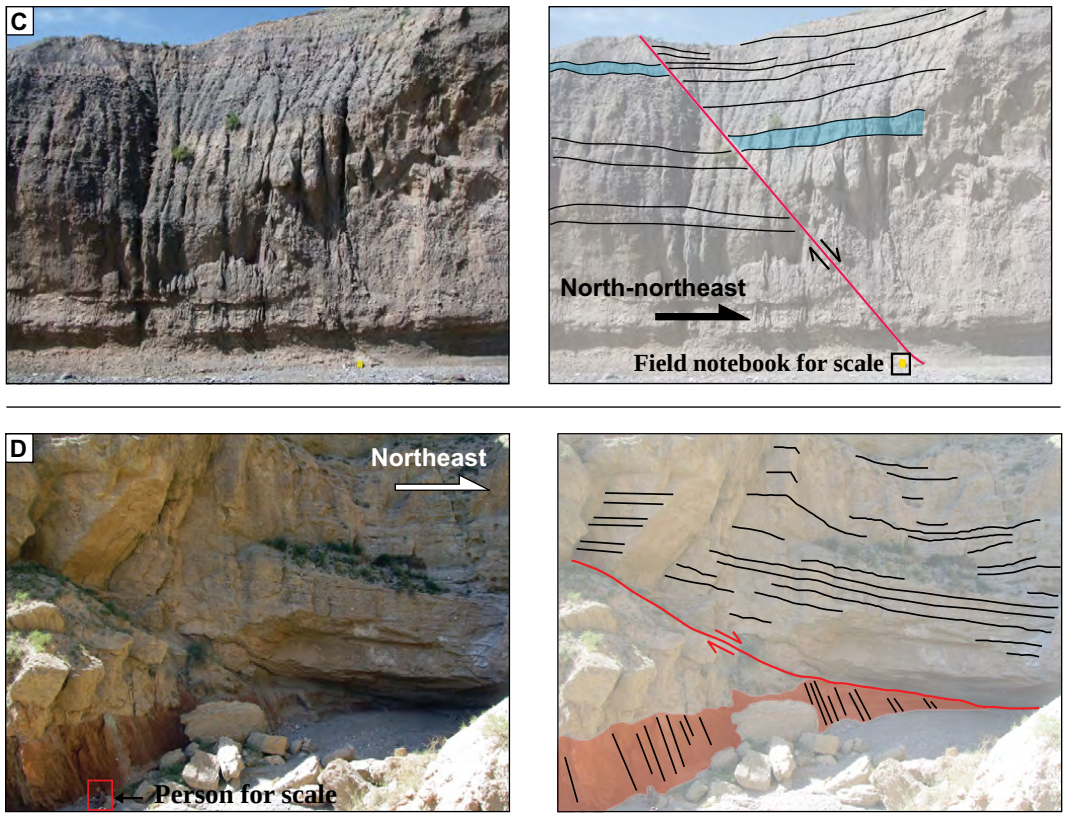

Figure 6 (*continued*). (C) Normal faulting of strata ~200 m north of the salt wall. (D) A large normal fault accommodating extension atop the Tuzimazha salt wall–salt thrust. The dip discordance may indicate that the normal fault localized along an unconformity separating different packages of halokinetic growth strata.

fabrics can be observed. These sites locally reveal a 1–3-m-thick rind along the top of the salt fountain in which mud is concentrated, presumably due to removal of halite via dissolution: these are hallmarks of cap-rock formation. Flow-band fabrics observed in the halite-dominated rock contrast with cm- to m-scale breccia blocks of mud-dominated strata (Fig. 8C). Bimodal grain size distributions are commonly observed in both fresh and weathered exposures of flow-banded halite (Fig. 8D). These size distributions likely reflect the transition from dislocation creep in the vent to grain size reduction via dissolution creep during surface and/or near-surface flow in the salt fountain (cf. Schleder and Urai, 2006; Urai and Spiers, 2007; Talbot and Pohjola, 2009).

DISCUSSION

Our field-based and satellite-image analysis provides first-order characterization of three km-scale surface salt structures of the western Kuqa fold-thrust belt. The Quele open-toed salt thrust sheet is marked by an active, advancing salt flow on a very broad front that features internal folding, salt-lined transfer fault structures, dissolution topography, flanking growth strata, and alluvial fan/stream-network interactions. The Tuzimazha salt wall also features flanking growth strata as well as flanking normal faults, and fluvial stream networks are deflected by the rising weak tabular salt body. The Awate salt fountain may be localized by the intersection of structures and/or the intersection of a thrust fault and a river. Alternatively, it may represent a long-lived diapir that influenced development of the structural and surface process systems, or some combination of these mechanisms may have generated the structure. We review the implications of our findings for related structural and surface processes in the following sections.

Surface Observations and Regional Structural Evolution

Most interpretations of regional structural evolution have been primarily derived from the mapping of Zhong and Xia (1998) and subsequent analysis of seismic reflection profiles and basin-scale growth strata geometries (e.g., Chen et al., 2004; Tang et al., 2004; Wang et al., 2011; Li et al., 2012). Surface observations of salt structures can further inform our understanding by affording direct observation of salt deformation mechanisms, relationships between salt and adjacent strata, and relationships between deformation and surface processes.

Our analysis of surface salt structures confirms that the western Kuqa fold-thrust belt experiences active deformation from foreland to hinterland. Active deformation along the strike of the Quilitage anticline system is evinced by the advancing flow of the Quele open-toed salt thrust sheet. Similarly, the topographic maximum provided by the Tuzimazha salt wall demonstrates active salt extrusion within the northern contractional belt. Meter-scale halokinetic growth strata record salt uplift at both Quele and Tuzimazha.

The observation that Kumugeliemu Group salt transitions laterally into bedded strata (Fig. 4D) helps refine our model understanding of the growth of the Quele open-toed salt thrust sheet. The Quele salt thrust may represent a thrust that nucleated within, and broke through, a former detachment fold (He and Li, 2009). Alternatively, the Quele salt thrust may have propagated from the position of a small Late Oligocene salt diapir, such that the thrust continues to separate strata north and south of the original diapir (Li et al., 2012). The key evidence cited in support of the second model is the lateral termination of Oligocene bedded strata by salt, as imaged in seismic profiles (Li et al., 2012). This termination is taken to represent a diapiric cut-off relationship. However, the field evidence documenting a gradual lateral transition from bedded strata

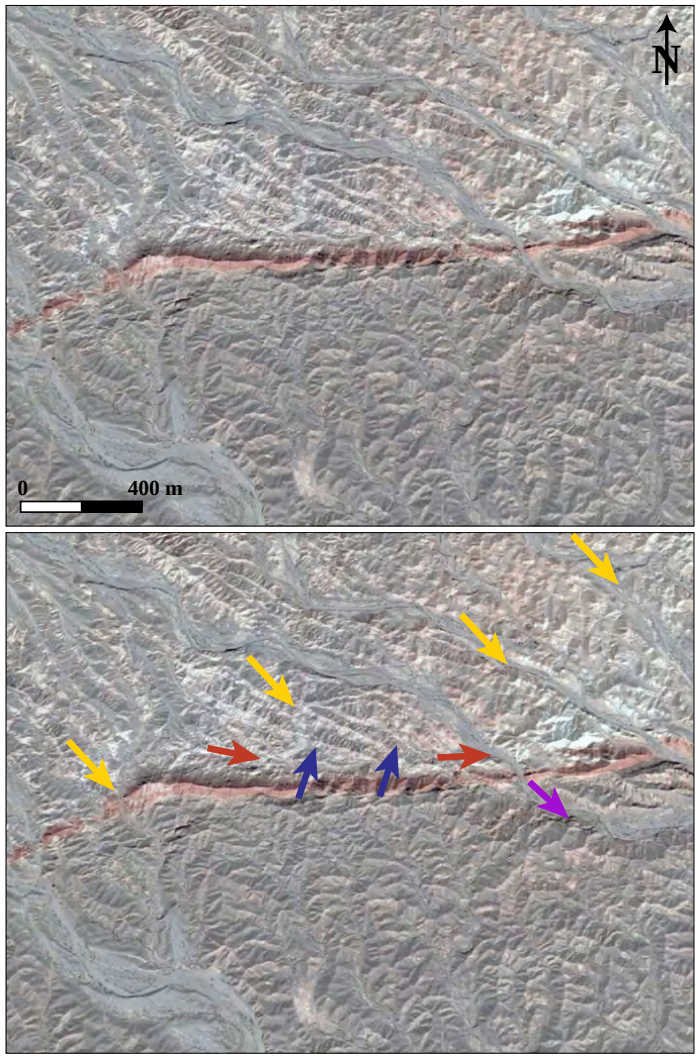

Figure 7. Satellite image showing the impact of Tuzimazha salt wall uplift on stream network morphology. Yellow arrows highlight the dominant regional stream-flow direction, to the southeast. Smaller streams are deflected by the rising salt wall and adjacent tilted strata (red arrows). Where the local high ridge separates from the salt wall, trending parallel to the wall but occurring ~50 m farther south, small streams flow back north across the salt wall (blue arrows). The purple arrow highlights the fate of streams large and small: with collection of sufficient stream power, all streams flow southeast.

to salt suggests an alternative interpretation, i.e., that similar transitions occurring at depth may be primary (sedimentary) structures. Compositional variability in the original deposits may lead to strength contrasts that allow some strata to break up and flow and other portions to remain cohesive (cf. Fiduk and Rowan, 2012). The terminations observed in seismic profiles do not require exclusive interpretation as cut-off relationships, and thus the broken detachment fold model for the Quele salt thrust remains viable.

Impacts of Surface Processes

Surface processes play important roles in shaping structural evolution, particularly in fold-thrust belts such as Kuqa, where growth strata comprise over 50% of the deformed material. Similarly, structural developments can affect drainage networks and other erosional systems; so the two sets of processes may interact. Across the Kuqa fold-thrust belt, drainage networks commonly can be correlated to structural grain; therefore, a key question is whether the drainage networks had a role in creating the structural grain. This appears to be the case for calving structures seen at the Awate salt fountain and Quele salt thrust sheet, where proximity to ephemeral water bodies correlates to the structural development (Figs. 4K and 9).

The Awate salt fountain may represent another example of fluvial systems impacting structural development. The Awate salt fountain appears to be a point-sourced salt structure, and it may represent a long-lived diapir. Alternatively, it may represent a response to a three-dimensional kinematic configuration that draws material up to a particular small region. As discussed above, this configuration could be entirely structurally controlled—a northwest-trending, salt-lined thrust fault passes through the region and may intersect with the northern termination of a north-trending strike-slip fault in the vicinity of the Awate salt fountain. Such a fault intersection could create a linear conduit along which salt might preferentially rise. However, it is not clear whether this strike-slip fault extends so far north. Another possibility is that a north-trending, southwards-flowing river directly west of the Awate salt fountain—and separating it from another namakier farther west—may have locally enhanced erosion along the salt-lined thrust, triggering focused exhumation of salt. In the latter interpretation, the Awate salt fountain may represent a salt tectonics equivalent to a river anticline or tectonic aneurysm (i.e., Zeitler et al., 2001; Montgomery and Stolar, 2006): a three-dimensional exhumation structure developed by the combination of belt-parallel shortening structures and belt-perpendicular focused erosion.

Prior work establishes that lateral growth of Quilitage anticline system folds and salt-cored detachment folds farther south is recorded by stream network morphology (He and Li, 2009). Our new observations of the Tuzimazha salt wall indicate similar impacts on stream network morphology, with additional complications due to rapid surface exhumation of weak salt. The local topographic high of the salt wall as well as the patterns of flanking growth strata and normal faulting indicate that the salt wall has the most rapid uplift in the vicinity. This generally results in deflections of small streams along the margin of the salt wall, but the high erodibility of the salt limits this effect. Where the salt erodibility trumps the rapid uplift, the local ridge occurs not along the salt wall, but rather in adjacent clastic sediment (Fig. 7). Here, streams are even directed back north across the salt wall against the regional flow direction. Therefore while the overall behavior mimics stream deflection in more common structural systems, such as the

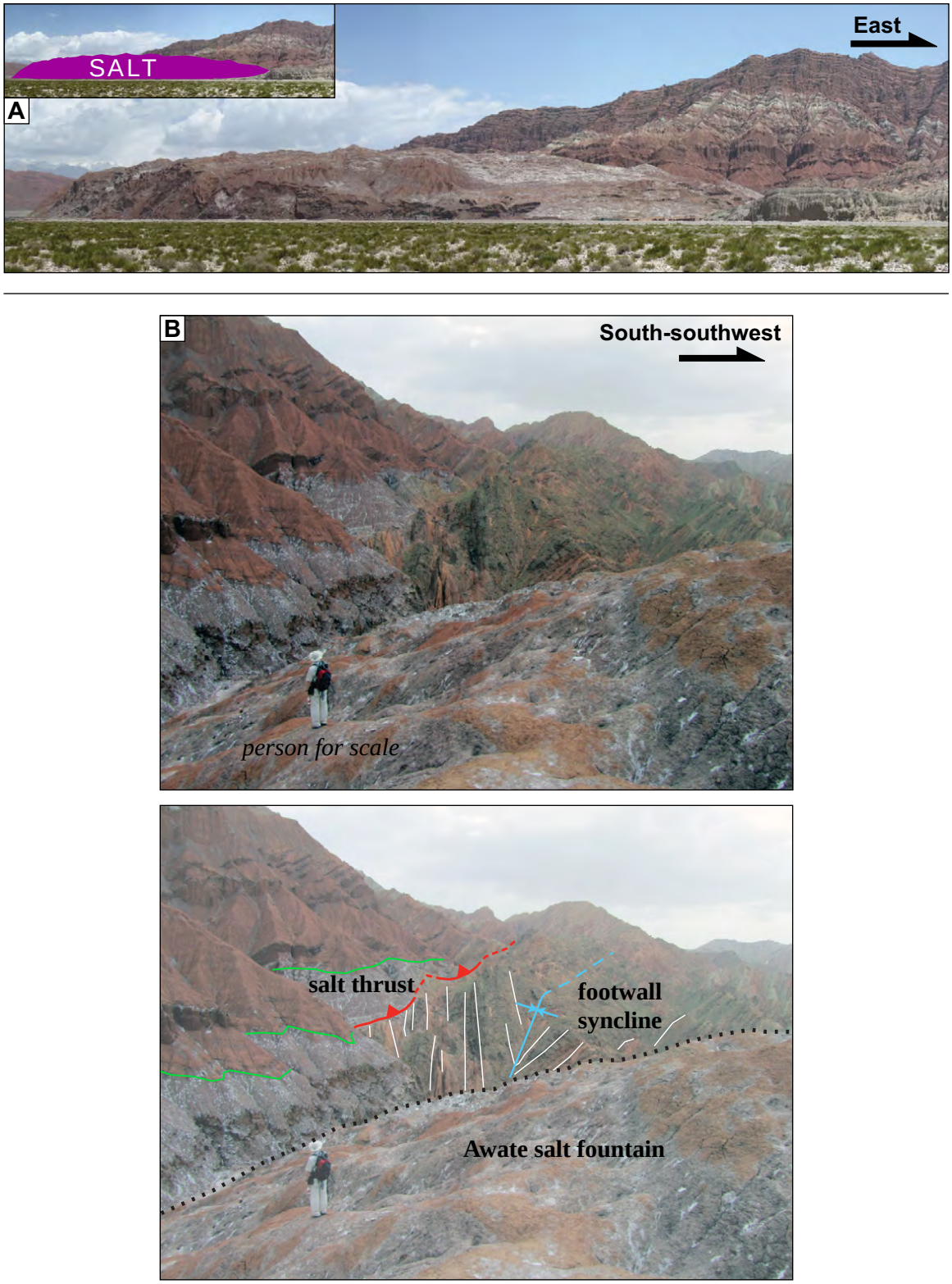

Figure 8 (*on this and following page*). Photographs of key features of the Awate salt fountain. Vantage points for photographs are indicated in Figures 1 and 3. (A) The Awate salt fountain, view looking north. The salt fountain locally exceeds 200 m in elevation above local base level. (B) A salt-lined thrust, footwall syncline, and a portion of the Awate salt fountain, as viewed looking east from the Awate salt fountain. The salt-lined thrust likely represents one of two or three intersecting features that together may localize salt uplift and generate the Awate salt fountain. The other features are a river (which could generate salt exhumation via localized erosion) and a strike-slip fault (see text for details).

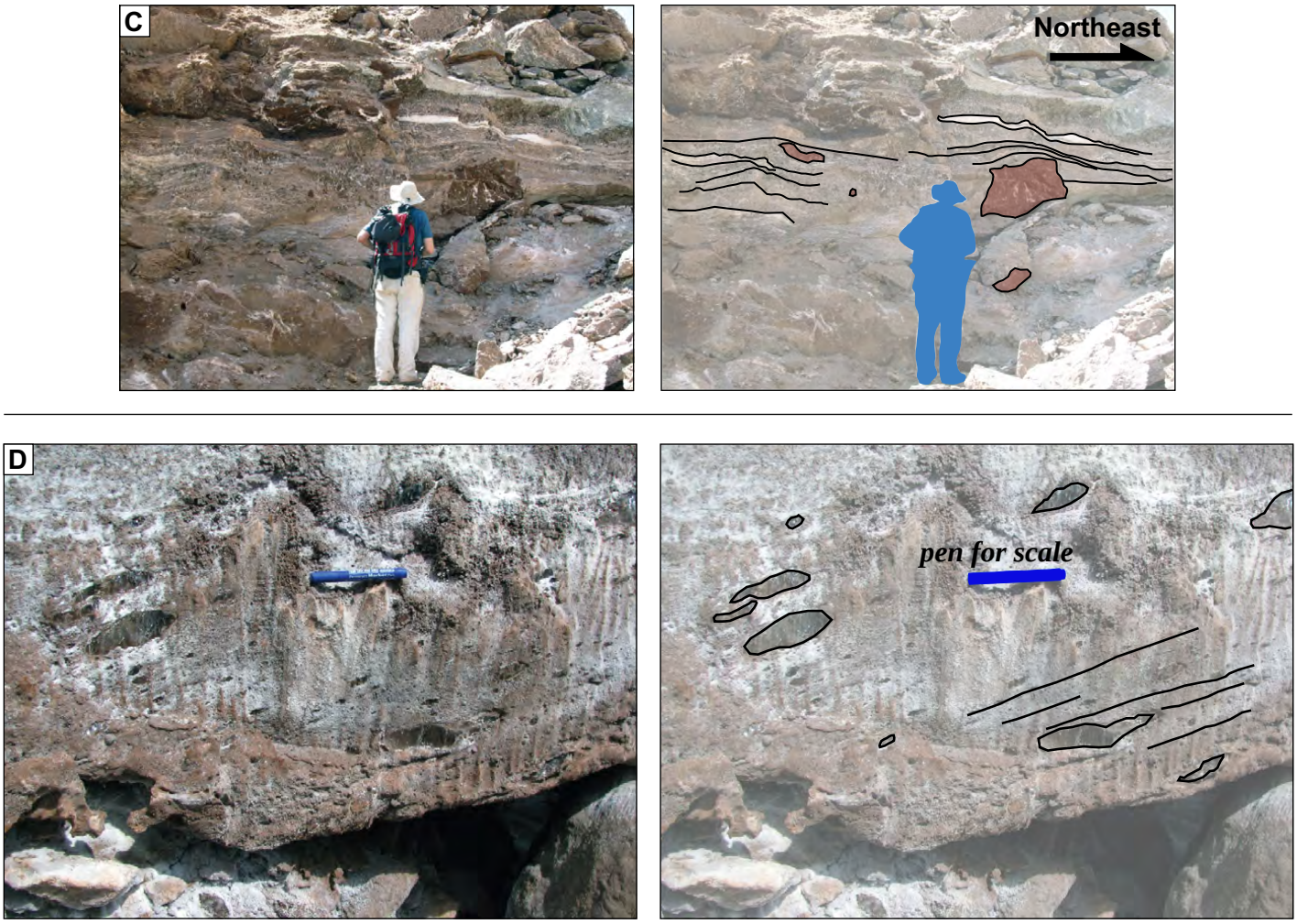

Figure 8 (*continued*). (C) Mining operations at the southern end of the Awate salt fountain commonly offer fresh exposures of salt as deep as ~30 m. Internal structure of the Awate salt fountain reveals ductile flow of salt enveloping brecciated block boudins of mudrock. (D) Float block that shows bimodal grain size distribution common to salt surface flows, with large grains recording dislocation creep in the vent and groundmass generated via dissolution creep during surface and/or near-surface flow.

lateral growth of anticlines (cf. Keller et al., 1998; He and Li, 2009), the impacts of relative erodibility are dramatically enhanced.

Implications for Future Work

The line-sourced salt structures of Kuqa represent some of the best active subaerial structures of this kind on Earth, and they will surely be a target of future salt tectonics research. The advantages of a locally plane strain background signal will allow along-strike differences in morphology to be explored in terms of second-order variations. The distinguishing low viscosity and high erodibility of the salt, in combination with a metronomic regional climatic signal of mild summer rains and otherwise sparse precipitation, indicate that these line-sourced structures may represent ideal sites to explore concepts of linked crustal channel flow– and climate-trigger–focused erosion (e.g., Beaumont et al., 2001; Hodges et al., 2001). New sites are required for such efforts because the Himalaya—the widely acknowledged representative example of such processes (e.g., Jamieson and Beaumont, 2013)—fails model tests and thus cannot have experienced significant crustal channel flow–focused erosion linkage (e.g., Webb et al., 2007, 2013; Leger et al., 2013). Similarly, as the site of some of Earth's most accessible high viscosity-contrast active structures, featuring interactions of ductile deformation and surface processes, the Kuqa fold-thrust belt may well serve as a training ground for geological exploration of other planets.

CONCLUSIONS

The western Kuqa fold-thrust belt represents a newly recognized laboratory for salt surface tectonics. Here, we provide a preliminary analysis of the geometry, kinematics, and surface processes of three surface salt structures. Two are line-sourced: the Quele open-toed salt thrust sheet and the Tuzimazha salt wall; the third—the Awate salt fountain—appears to be point-sourced. All of these structures display active exhumation of salt, demonstrating that active deformation occurs from the foreland to the hinterland of the Kuqa fold-thrust belt. In addition to fold and growth strata development, the Kuqa surface salt structures display a variety of interactions with surface processes. These include dissolution topography, calving structures,

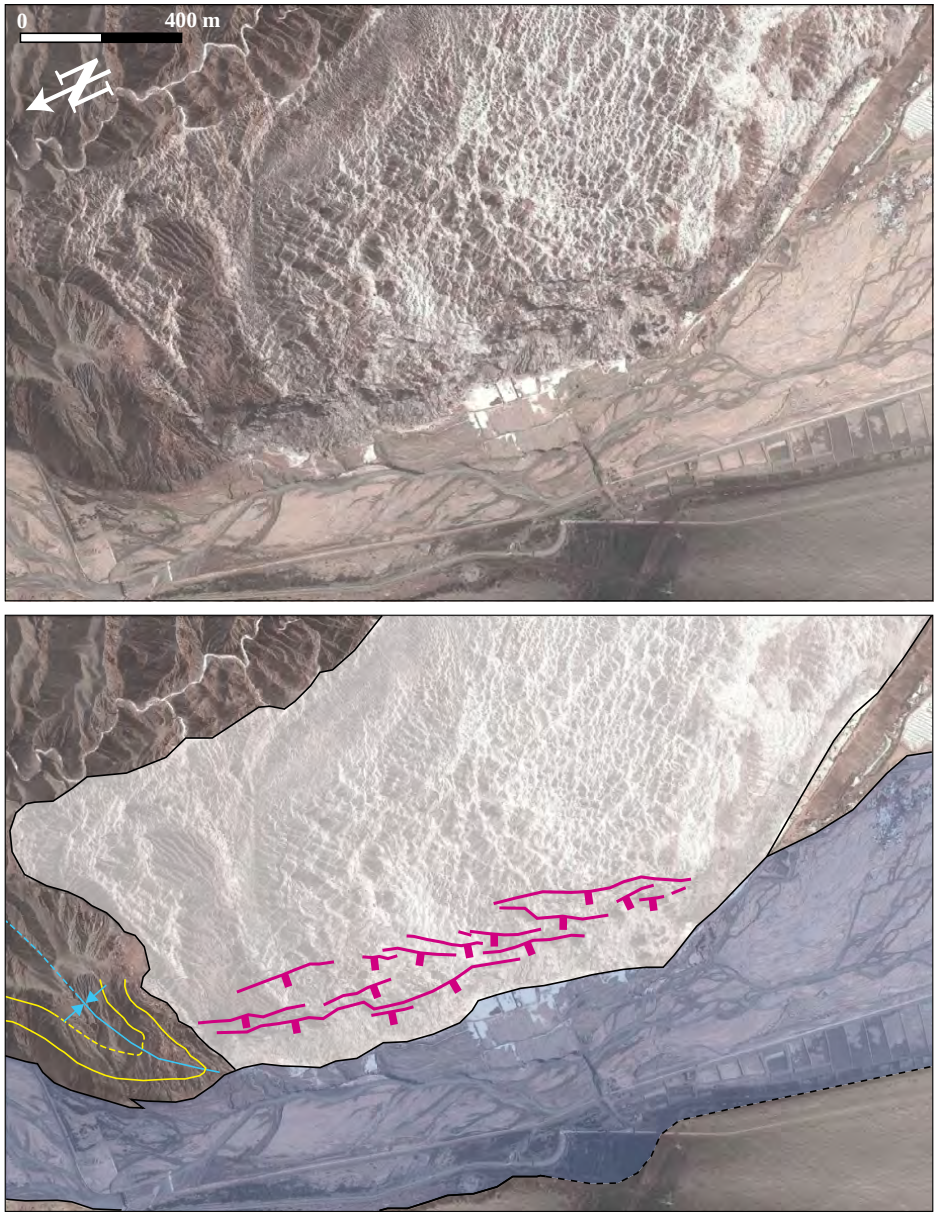

Figure 9. Satellite image showing calving structures along the western edge of the Awate salt fountain. The calving structures exclusively develop in the salt near the main channel and floodplain of the adjacent river, suggesting a causal link between fluid infiltration and salt weakening and/or calving.

stream deflections, and possibly even the salt tectonics equivalent to a tectonic aneurysm (cf. Zeitler et al., 2001).

ACKNOWLEDGMENTS

Christopher Talbot provided a wealth of generous feedback during our preparation of this manuscript. We thank Chris, Mark Rowan, and Associate Editor Katherine Giles for constructive reviews that were instrumental in sharpening interpretations and communication and Shanaka de Silva for his editorial guidance and persistence. This work is supported by the Tarim Oil Company, a subsidiary of the China National Petroleum Corporation and by grants from the American Chemical Society's Petroleum Research Fund (PRF-53549-ND8) and the Tectonics program of the U.S. National Science Foundation (EAR-1322033).

REFERENCES CITED

Allen, M.B., Windley, B.F., Chi, Z., Zhong-Yan, Z., and Guang-Rei, W., 1991, Basin evolution within and adjacent to the Tien Shan Range, NW China: Journal of the Geological Society of London, v. 148, no. 2, p. 369–378, doi:10.1144/gsjgs.148.2.0369.

Barnhart, W.D., and Lohman, R.B., 2012, Regional trends in active diapirism revealed by mountain range-scale InSAR time series: Geophysical Research Letters, v. 39, no. 8, doi:10.1029/2012GL051255.

Beaumont, C., Jamieson, R.A., Nguyen, M.H., and Lee, B., 2001, Himalayan tectonics explained by extrusion of a low-viscosity crustal channel coupled to focused surface denudation: Nature, v. 414, p. 738–742, doi:10.1038/414738a.

Charreau, J., Gilder, S., Chen, Y., Dominguez, S., Avouac, J.-P., Sen, S., and Wang, W., 2006, Magnetostratigraphy of the Yaha section, Tarim Basin (China): 11 Ma acceleration in erosion and uplift of the Tian Shan mountains: Geology, v. 34, no. 3, p. 181, doi:10.1130/G22106.1.

Chen, S., Tang, L., Jin, Z., Jia, C., and Pi, X., 2004, Thrust and fold tectonics and the role of evaporites in deformation in the Western Kuqa Foreland of Tarim Basin, Northwest China: Marine and Petroleum Geology, v. 21, no. 8, p. 1027–1042, doi:10.1016/j.marpetgeo.2004.01.008.

Craig, T., Copley, A., and Jackson, J., 2012, Thermal and tectonic consequences of India underthrusting Tibet: Earth and Planetary Science Letters, v. 353–354, p. 231–239, doi:10.1016/j.epsl.2012.07.010.

Dribus, J.R., Jackson, M.P.A., Kapoor, J., and Smith, M.F., 2008, The prize beneath the salt: Oilfield Review, v. 15, p. 4–17.

Fiduk, J.C., and Rowan, M.G., 2012, Analysis of folding and deformation within layered evaporites in Blocks BM-S-8 & 9, Santos Basin, Brazil, *in* Alsop, I.A., Archer, S.G., Hartley, A.J., Grant, N.T., and Hodgkinson, R., eds., Salt Tectonics, Sediments and Prospectivity: Geological Society of London Special Publication 363, p. 471–487.

Giles, K.A., and Rowan, M.G., 2012, Concepts in halokinetic-sequence deformation and stratigraphy, *in* Alsop, I.A., Archer, S.G., Hartley, A.J., Grant, N.T., and Hodgkinson, R., eds., Salt Tectonics, Sediments and Prospectivity: Geological Society of London Special Publication 363, p. 7–31.

He, D., and Li, J., 2009, Drainage network development and fold growth of Quilitage structural belt in the Kuqa foreland fold and thrust belt: Acta Geologica Sinica, v. 83, p. 1074–1082.

Hendrix, M.S., Graham, S.A., Carroll, A.R., Sobel, E.R., McKnight, C.L., Schulein, B.J., and Wang, Z., 1992, Sedimentary record and climatic implications of recurrent deformation in the Tian Shan: Evidence from Mesozoic strata of north Tarim, south Junggar, and Turpan basins, northwest China: Geological Society of America Bulletin, v. 104, p. 53–79, doi:10.1130/0016-7606(1992)104<0053:SRACIO>2.3.CO;2.

Hodges, K.V., Hurtado, J.M., and Whipple, K.X., 2001, Southward extrusion of Tibetan crust and its effect on Himalayan tectonics: Tectonics, v. 20, p. 799–809, doi:10.1029/2001TC001281.

Huang, B., Piper, J.D.A., Peng, S., Liu, T., Li, Z., Wang, Q., and Zhu, R., 2006, Magnetostratigraphic study of the Kuche Depression, Tarim Basin, and Cenozoic uplift of the Tian Shan Range, Western China: Earth and Planetary Science Letters, v. 251, p. 346–364, doi:10.1016/j.epsl.2006.09.020.

Hubert-Ferrari, A., Suppe, J., Gonzalez-Mieres, R., and Wang, X., 2007, Mechanisms of active folding of the landscape (southern Tian Shan, China): Journal of Geophysical Research, v. 112, no. B3, doi:10.1029/2006JB004362.

Hudec, M.R., and Jackson, M.P.A., 2006, Advance of allochthonous salt sheets in passive margins and orogens: American Association of Petroleum Geologists Bulletin, v. 90, no. 10, p. 1535–1564, doi:10.1306/05080605143.

Hudec, M.R., and Jackson, M.P.A., 2007, Terra infirma: Understanding salt tectonics: Earth-Science Reviews, v. 82, no. 1–2, p. 1–28, doi:10.1016/j.earscirev.2007.01.001.

Hudec, M.R., and Jackson, M.P.A., 2011, The Salt Mine: A Digital Atlas of Salt Tectonics: The University of Texas at Austin, Bureau of Economic Geology, Udden Book Series No. 5, American Association of Petroleum Geologists Memoir 99, 305 p.

Jamieson, R.A., and Beaumont, C., 2013, On the origin of orogens: Geological Society of America Bulletin, v. 125, p. 1671–1702, doi:10.1130/B30855.1.

Jin, Z.-M., Green, H.W., and Zhou, Y., 1994, Melt topology in partially molten mantle peridotite during ductile deformation: Nature, v. 372, p. 164–167, doi:10.1038/372164a0.

Keller, E.A., Zepeda, R.L., Rockwell, T.K., Ku, T.L., and Dinklage, W.S., 1998, Active tectonics at Wheeler Ridge, southern San Joaquin Valley, California: Geological Society of America Bulletin, v. 110, p. 298–310, doi:10.1130/0016-7606(1998)110<0298:ATAWRS>2.3.CO;2.

Leger, R.M., Webb, A.A.G., Henry, D.J., Craig, J.A., and Dubey, P., 2013, Metamorphic field gradients across the Himachal Himalaya, northwest India: Implications for the emplacement of the Himalayan crystalline core: Tectonics, v. 32, p. 540–557, doi:10.1002/tect.20020.

Letouzey, J., Colletta, B., Vially, R., and Chermette, J.C., 1995, Evolution of salt-related structures in compressional settings, *in* Jackson, M.P.A., Roberts, D.G., and Snelson, S., eds., Salt Tectonics: A Global Perspective: American Association of Petroleum Geologists Memoir 65, p. 41–60.

Li, S., Wang, X., and Suppe, J., 2012, Compressional salt tectonics and synkinematic strata of the western Kuqa foreland basin, southern Tian Shan, China: Basin Research, v. 24, no. 4, p. 475–497, doi:10.1111/j.1365-2117.2011.00531.x.

Mann, P., Gahagan, L., and Gordon, M.B., 2003, Tectonic setting of the world's giant oil and gas fields, *in* Halbouty, M.T., ed., Giant Oil and Gas Fields of the Decade, 1990–1999: American Association of Petroleum Geologists Memoir, v. 78, p. 15–105.

McClay, K., Muñoz, J.-A., and Senz, J.G., 2004, Extensional salt tectonics in a contractional orogen: A newly identified tectonic event in the Spanish Pyrenees: Geology, v. 32, no. 9, p. 737–740.

McEwen, A.S., Ojha, L., Dundas, C.M., Mattson, S.S., Byrne, S., Wray, J.J., Cull, S.S., Murchie, S.L., Thomas, N., and Gulick, V.C., 2011, Seasonal flows on warm Martian slopes: Science, v. 333, p. 740–743, doi:10.1126/science.1204816.

McKenzie, D., Ford, P.G., Liu, F., and Pettengill, G.H., 1992, Pancakelike domes on Venus: Journal of Geophysical Research, v. 97, no. E10, p. 15,967–15,976, doi:10.1029/92JE01349.

Molnar, P., and Tapponnier, P., 1975, Cenozoic tectonics of Asia: Effects of a continental collision: Science, v. 189, no. 4201, p. 419–426, doi:10.1126/science.189.4201.419.

Montgomery, D.R., and Stolar, D.B., 2006, Reconsidering Himalayan river anticlines: Geomorphology, v. 82, p. 4–15, doi:10.1016/j.geomorph.2005.08.021.

Montgomery, D.R., Som, S.M., Jackson, M.P.A., Schreiber, B.C., Gillespie, A.R., and Adams, J.B., 2009, Continental-scale salt tectonics on Mars and the origin of Valles Marineris and associated outflow channels: Geological Society of America Bulletin, v. 121, p. 117–133.

Peng, S., Li, Z., Huang, B., Liu, T., and Wang, Q., 2006, Magnetostratigraphic study of Cretaceous depositional succession in the northern Kuqa Depression, Northwest China: Chinese Science Bulletin, v. 51, p. 97–107, doi:10.1007/s11434-005-0340-5.

Rowan, M.G., and Vendeville, B.C., 2006, Foldbelts with early salt withdrawal and diapirism: Physical model and examples from the northern Gulf of Mexico and the Flinders Ranges, Australia: Marine and Petroleum Geology, v. 23, p. 871–891, doi:10.1016/j.marpetgeo.2006.08.003.

Rowan, M.G., Lawton, T.F., and Giles, K.A., 2012, Anatomy of an exposed vertical salt weld and flanking strata, La Popa Basin, Mexico, *in* Alsop, I.A., Archer, S.G., Hartley, A.J., Grant, N.T., and Hodgkinson, R., eds., Salt Tectonics, Sediments and Prospectivity: Geological Society of London Special Publication 363, p. 33–57.

Schleder, Z., and Urai, J.L., 2006, Deformation and recrystallization mechanisms in mylonitic shear zones in naturally deformed extrusive Eocene–Oligocene rock salt from Eyvanekey plateau and Garmsar hills (central Iran): Journal of Structural Geology, v. 29, p. 2241–2255.

Spetzler, H., and Anderson, D.L., 1968, The effect of temperature and partial melting on velocity and attenuation in a simple binary system: Journal of Geophysical Research, v. 73, no. 18, p. 6051–6060, doi:10.1029/JB073i018p06051.

Sun, J., Li, Y., Zhang, Z., and Fu, B., 2009, Magnetostratigraphic data on Neogene growth folding in the foreland basin of the southern Tianshan Mountains: Geology, v. 37, p. 1051–1054, doi:10.1130/G30278A.1.

Talbot, C.J., 1998, Extrusions of Hormuz salt in Iran: Geological Society of London Special Publication no. 1, p. 315–334, doi:10.1144/GSL.SP.1998.143.01.21.

Talbot, C.J., and Pohjola, V., 2009, Subaerial salt extrusions in Iran as analogues of ice sheets, streams and glaciers: Earth-Science Reviews, v. 97, p. 155–183, doi:10.1016/j.earscirev.2009.09.004.

Tang, L.-J., Jia, C.-Z., Jin, Z.-J., Chen, S.-P., Pi, X.-J., and Xie, H.-W., 2004, Salt tectonic evolution and hydrocarbon accumulation of Kuqa foreland fold belt, Tarim Basin, NW China: Journal of Petroleum Science Engineering, v. 41, no. 1–3, p. 97–108, doi:10.1016/S0920-4105(03)00146-3.

Thoms, R.L., and Gehle, R.M., 2000, A brief history of salt cavern use: College Station, Texas, AGM, Inc., 8 p.

Urai, J.L., and Spiers, C.J., 2007, The effect of grain boundary water on deformation mechanisms and rheology of rock salt during long-term deformation, *in* Wallner, M., Lux, K., Minkley, W., and Hardy, H., Jr., eds., The Mechanical Behavior of Salt—Understanding of THMC Processes in Salt: Hannover, Germany, p. 149–158.

Wang, Q., Zhang, P.-Z., Freymueller, J.T., Bilham, R., Larson, K.M., Lai, X., You, X., Niu, Z., Wu, J., Li, Y., Liu, J., Yang, Z., and Chen, Q., 2001, Present-day crustal deformation in China constrained by Global Positioning System measurements: Science, v. 294, p. 574–577, doi:10.1126/science.1063647.

Wang, X., Suppe, J., Guan, S., Hubert-Ferrari, A., Gonzalez-Mieres, R., and Jia, C., 2011, Cenozoic structure and tectonic evolution of the Kuqa fold belt, southern Tian Shan, China, *in* McClay, K., Shaw, J.H., and Suppe, J., eds., Thrust Fault-Related Folding: American Association of Petroleum Geologists Memoir 94, p. 215–243.

Warren, J.K., 2006, Evaporites: Sediments, Resources and Hydrocarbons: Berlin, Springer, 1036 p.

Webb, A.A.G., Yin, A., Harrison, T.M., Célérier, J., and Burgess, W.P., 2007, The leading edge of the Greater Himalayan crystallines revealed in the NW Indian Himalaya: Implications for the evolution of the Himalayan orogen: Geology, v. 35, no. 10, p. 955–958, doi:10.1130/G23931A.1.

Webb, A.A.G., Yin, A., and Dubey, C.S., 2013, U-Pb zircon geochronology of major lithologic units in the Eastern Himalaya: Implications for the origin and assembly of Himalayan rocks: Geological Society of America Bulletin, v. 125, p. 499–522, doi:10.1130/B30626.1.

Yin, A., Nie, S., Craig, P., Harrison, T.M., Ryerson, F.J., Xianglin, Q., and Geng, Y., 1998, Late Cenozoic tectonic evolution of the southern Chinese Tian Shan: Tectonics, v. 17, no. 1, p. 1–27, doi:10.1029/97TC03140.

Zeitler, P.K., Koons, P.O., Bishop, M.L., Chamberlain, C.P., Craw, D., Edwards, M.A., Hamidullah, S., Jan, M.Q., Khan, M.A., Khattak, M.U.K., Kidd, W.S.F., Mackie, R.L., Meltzer, A.S., Park, S.K., Pecher, A., Poage, M.A., Sarker, G., Schneider, D.A., Seeber, L., and Shroder, J., 2001, Crustal reworking at Nanga Parbat, Pakistan: Evidence for erosional focusing of crustal strain: Tectonics, v. 20, p. 712–728, doi:10.1029/2000TC001243.

Zhao, W., Zhang, S., Wang, F., Cramer, B., Chen, J., Sun, Y., and Zhao, M., 2005, Gas systems in the Kuche Depression of the Tarim Basin: Source rock distributions, generation kinetics and gas accumulation history: Organic Geochemistry, v. 36, p. 1583–1601, doi:10.1016/j.orggeochem.2005.08.016.

Zhong, D., and Xia, W.S., (1998). The investigation report of Mesozoic–Cenozoic strata, structure, sedimentary faces, and petroleum potential of Kuche foreland basin outcrop area (with 1:100,000 Kuche foreland basin geologic map) (in Chinese with English abstract): Xinjiang, Research report of Tarim Oilfield Company, 462 p.

Zubovich, A.V., Wang, X.Q., Scherba, Y.G., Schelochkov, G.G., Reilinger, R., Reigber, C., Mosienko, O.I., Molnar, P., Michajljow, W., Makarov, V.I., Li, J., Kuzikov, S.I., Herring, T.A., Hamburger, M.W., Hager, B.H., Dang, Y., Bragin, V.D., and Beisenbaev, R.T., 2010, GPS velocity field for the Tien Shan and surrounding regions: Tectonics, v. 29, doi:10.1029/2010TC002772.